Two-parameter study of square-wave switching dynamics in orthogonally delay-coupled semiconductor lasers

C. Masoller[1], M. Sciamanna[2], A. Gavrielides[3],
[1] *Departament de Fisica i Enginyeria Nuclear, Universitat Politecnica de Catalunya, Colom 11, E-08222 Terrassa, Barcelona, Spain,*
[2] *Optics and Electronics (OPTEL) Research Group, Laboratoire Matériaux Optiques, Photonique et Systemes (LMOPS), Supélec, 2 Rue Edouard Belin, 57070 Metz, France,*
[3] *Air Force Research Laboratory, AFR/EOARD, 86 Blenheim Crescent,Ruislip Middlesex HA4 7HB, United Kingdom*
(Dated: March 13, 2013)

We perform a detailed numerical analysis of square-wave polarization switching in two semiconductor lasers with time-delayed, orthogonal mutual coupling. An in-depth mapping of the dynamics in the two-parameter plane coupling strength versus frequency detuning shows that stable square-waves occur in narrow parameter regions that are localized close to the boundary of stability of the pure-mode solution. In this steady state the two coupled lasers emit orthogonal polarizations. We also show that there are various types of square-wave forms and that stable switching does not need the inclusion of noise or nonlinear gain in the model. As these narrow regions of deterministic and stable square waves occur for quite different combinations of parameters, they could potentially explain the waveforms that have been observed experimentally. However, on the other hand, these regions are narrow enough to be in fact considered as experimentally unreachable. Therefore, our results indicate that further experimental statistical studies are needed in order to distinguish deterministic and stationary square waveforms from long transients due to noise.

I. INTRODUCTION

Recent years have seen an increased interest in understanding the physics and bifurcations at the origin of self-pulsating dynamics in a laser diode with time-delayed optical feedback or coupling. The increase of the feedback/coupling strength typically destabilizes the otherwise steady dynamics to self-pulsation with a period either close to the laser relaxation oscillation frequency or to the feedback/coupling delay time [1]. The waveform can vary from sharp pulsing to harmonic to square-wave depending on the system non-linearity [2–5], on the sub- or super-critical nature of the underlying Hopf bifurcation [5, 6], on the laser mode competition or on the coupling/feedback parameters [7–15]. An interesting combination of these parameters is found in a recent experiment, where two edge-emitting laser diodes are mutually coupled through their orthogonal polarization modes [16]. Depending on the coupling strength and delay and on the mode competition (gain/loss ratio), the laser dynamics shows square waveforms with different time-period and duty cycle. The dynamics has been reproduced numerically by a two-mode rate equation model with time-delayed coupling including gain saturation and frequency detuning [17]. Although the dynamics has been initially thought to be driven by noise, the numerical study has shown that square waveforms can be observed also in the deterministic model. The bifurcation at the origin of the square-wave dynamics has been very recently elucidated thanks to advanced continuation techniques [18]. The bifurcation study has confirmed the deterministic scenario leading to square-wave dynamics: square-waveforms result from a cascade of Hopf bifurcations on a two-mode steady-state and become stable only in a narrow interval of the coupling strength close to a transcritical bifurcation to a one-mode steady-state solution. Previous works however have raised additional questions, e.g., how do the results depend on the model additional parameters such as gain saturation and detuning, and can we find a larger region of parameters where to observe stable square-wave dynamics?

We address here these pending issues on a system made of two laser diodes with delayed-coupling of their orthogonal polarization modes. We complement our earlier numerical and bifurcation studies by an in-depth analysis of the dynamics in the two-parameter plane coupling strength versus frequency detuning and for different values of the gain saturation coefficients. We find several interesting new conclusions: 1) stable square-waves always occur in narrow ranges of the coupling strength and detuning parameters close to the transition to the one-mode (pure mode) steady-state, but we find many such intervals of stable square-waves in the whole parameter space, 2) stable square-waves can be observed also when the gain saturation coefficients are equal to zero, although in that case the square wave dynamics acquire a fast weakly damped oscillation at the relaxation frequency of the laser in addition to the fundamental modulation at the coupling delay time, 3) noise-free simulations show regions of parameters with stable square-waves that are otherwise suppressed when including noise, hence suggesting coexistence of several other attractors. Our work brings therefore new light into the parameters leading to square-wave switching dynamics and motivates additional bifurcation studies in the two parameter plane coupling strength versus frequency detuning.

Our paper is organized as follows. Section II details the rate equation model and parameters, as well as the steady-states and their stability. Our numerical results on the mapping of the dynamics in the two-parameter plane are shown in Sec. III. Our main conclusions are summarized in Sec. IV.

II. MODEL

A. Model equations

The rate-equations describing two identical semiconductor lasers mutually coupled through polarization-rotated optical injection are

$$\frac{dE_{x,i}}{dt} = k(1+j\alpha)(g_{x,i}-1)E_{x,i} + \sqrt{\beta_{sp}}\xi_{x,i}, \tag{1}$$

$$\frac{dE_{y,i}}{dt} = j\delta E_{y,i} + k(1+j\alpha)(g_{y,i}-1-\beta)E_{y,i} \tag{2}$$

$$+ \eta E_{x,3-i}(t-\tau) + \sqrt{\beta_{sp}}\xi_{y,i}, \tag{3}$$

$$\frac{dN_i}{dt} = \gamma_N[\mu - N_i - g_{x,i}I_{x,i} - g_{y,i}I_{y,i})]. \tag{4}$$

Here $i = 1$ and $i = 2$ denote the two lasers, E_x and E_y are orthogonal linearly polarized slowly-varying complex amplitudes (corresponding respectively to TE and TM polarizations) and N is the carrier density. In the absence of optical coupling the emission frequency of the two lasers is the same and is the frequency of the x polarization that is taken as reference frequency, with δ being the angular frequency detuning between the x and y polarizations. The

modal gains are:

$$g_{x,i} = N_i/(1 + \epsilon_{xx} I_{x,i} + \epsilon_{xy} I_{y,i}), \tag{5}$$
$$g_{y,i} = N_i/(1 + \epsilon_{yx} I_{x,i} + \epsilon_{yy} I_{y,i}). \tag{6}$$

Other parameters are: k is the field decay rate, γ_N is the carrier decay rate, α the linewidth enhancement factor, β is the linear loss anisotropy, β_{sp} is the noise strength, $\xi_{x,y}$ are uncorrelated Gaussian white noises and μ is the injection current parameter, normalized such that the solitary threshold is at $\mu_{th} = 1$. The parameters of the polarization-orthogonal mutual coupling are η and τ, which represent the coupling strength and the delay time respectively.

B. Steady state solutions

The model has two types of steady states:

(a) Mixed-mode solution, in which the two coupled lasers emit the x and y polarizations simultaneously, with

$$I_{1x} = I_{2x} = I_x, \tag{7}$$
$$I_{1y} = I_{2y} = I_y, \tag{8}$$
$$N_1 = N_2 = N. \tag{9}$$

I_x, I_y and N can be calculated from the following coupled set of equations for I_x, I_y and g_y:

$$\mu - 1 - (1 + \epsilon_{xx}) I_x - \epsilon_{xy} I_y - g_y I_y = 0, \tag{10}$$

$$g_y = \frac{1 + \epsilon_{xx} I_x + \epsilon_{xy} I_y}{1 + \epsilon_{yx} I_x + \epsilon_{yy} I_y}, \tag{11}$$

and

$$\eta^2 = \frac{I_y}{I_x} \left([\delta + k\alpha(g_y - 1 - \beta)]^2 + k^2 (g_y - 1 - \beta)^2 \right). \tag{12}$$

Equation (10) results from setting the time derivative of the carried density equal to zero, and eliminating N with $N = 1 + \epsilon_{xx} I_x + \epsilon_{xy} I_y$ (that results from $g_x = 1$). Equation (11) is obtained from Eqs. (5) and (6) using $g_x = 1$ and $N_1 = N_2 = N$. Equation (12) results from solving the field rate equations taking into account that the frequency of the y-polarization locks to the frequency of the injected x-polarization.

The procedure to solve these equations is as follows. Given $I_y > 0$, I_x is calculated from Eq. (10): by substituting g_y using Eq. (11), $I_x > 0$ is a solution of a second-order polynomial on I_y. With I_x and I_y, then g_y is calculated from Eq. (11), the coupling strength, η, from Eq. (12), and the carrier density from $N = 1 + \epsilon_{xx} I_x + \epsilon_{xy} I_y$.

(b) Pure-mode solution, in which one laser emits the x polarization while the other laser emits the y polarization. The coupling between the lasers in this solution is unidirectional, the laser that emits the x polarization acts as "master" laser, and the laser that emits the y polarization acts as "injected" laser.

For the master (solitary) laser the trivial steady state is:

$$I_x = \frac{\mu - 1}{1 + \epsilon_{xx}}, \tag{13}$$
$$N_x = 1 + \epsilon_{xx} I_x. \tag{14}$$

For the injected laser, the intensity and carrier density, I_y and N_y, can be calculated from two coupled equations for I_y and g_y,

$$\mu - g_y (1 + \epsilon_{yy} I_y) - g_y I_y = 0, \tag{15}$$

and

$$\eta^2 = \frac{I_y}{I_x} \left([\delta + k\alpha(g_y - 1 - \beta)]^2 + k^2 (g_y - 1 - \beta)^2 \right). \tag{16}$$

These equations are obtained in the same way as for the mixed mode solution (i.e. by setting the time derivative of the carried density equal to zero, and by solving the field rate equations taking into account that the frequency of the y-polarization locks to the frequency of the injected x-polarization). In Eq. (15) we used

$$g_y = \frac{N_y}{1 + \epsilon_{yy} I_y}. \tag{17}$$

to eliminate N_y.

The procedure to solve the coupled equations is the same as that described for the mixed mode solution: given $I_y > 0$ we compute g_y from Eq. (15). With g_y and I_x [calculated from Eq. (13)] we obtain the coupling strength from Eq. (16) and the carrier density from Eq. (17).

For typical parameter values, with $I_x, I_y > 0$ there is only one mixed-mode solution, and either one or three pure-mode solutions, depending on the coupling strength.

C. Stability of the steady states

The stability of the pure-mode and mixed-mode solutions was analyzed in [17, 18] and here we present a brief summary of the main results.

Since the pure-mode solution corresponds to a unidirectional coupling situation, in which there is no back delayed coupling from the injected laser to the master laser, its stability depends on the coupling strength, η, but does not depend on the delay time of the coupling, τ. For increasing η the pure mode undergoes a bifurcation that is of transcritical type due to a change of sign of a real eigenvalue [18]. The bifurcation occurs at a value of the coupling strength, η_c, that can be calculated from Eq. (16) with I_x and g_y calculated from Eqs. (13) and (17), and $I_y > 0$ being a solution of the polynomial equation

$$\epsilon_{xy}(1+\epsilon_{yy})I_y^2 + [1-(\mu-1)\epsilon_{yy}+\epsilon_{xy}]I_y - (\mu-1) = 0. \tag{18}$$

In addition, the pure-mode solution can undergo a Hopf bifurcation that brings time-dependent solutions with a frequency close to the laser relaxation oscillation.

The mixed mode becomes unstable after a supercritical Hopf bifurcation, after which symmetric ($I_{1x} = I_{2x}$, $I_{1y} = I_{2y}$, $N_1 = N_2$) time-dependent solutions emerge, with a frequency also close to the relaxation oscillation. At higher coupling strengths, several Hopf bifurcations of the now unstable mixed state occur. These bifurcations give rise to time-periodic solutions that are initially unstable, but they can become stable at larger coupling strengths, in narrow intervals of the coupling η. The periodicity of these initially unstable solutions grows with the coupling and at large η, unstable square-wave solutions emerge from Hopf bifurcations of the unstable mixed state, that have a periodicity close to the delay τ or close to 2τ. These solutions can latter become stable, at higher values of η, in narrow intervals of η values.

The analysis done in Ref. [18] (by employing continuation methods, and also numerically, by simulating the model equations), demonstrated that these square-wave solutions do not need and are not supported by the addition of noise, but are stable only in narrow parameter regions. In contrast, in Ref. [16], using a simpler model (without gain saturation and without frequency detuning) only transient square-wave dynamics were found. An interesting issue that remains to be investigated is to which extent the stability of square-wave dynamics depends on these parameters, and if there is any role of the noise. In the next section we address these issues by presenting the results of extended numerical simulations of the model equations, displaying different types of square-wave switching dynamics.

III. NUMERICAL RESULTS

The simulation of the model equations were carried out considering the same parameters as in [17, 18], unless otherwise explicitly indicated: $k = 300$ ns^{-1}, $\mu = 2$, $\alpha = 3$, $\gamma_N = 0.5$ ns^{-1}, $\beta = 0.04$, $\epsilon_{xx} = 0.01$, $\epsilon_{xy} = 0.015$, $\epsilon_{yx} = 0.02$, $\epsilon_{yy} = 0.025$, $\beta_{sp} = 10^{-5}$ ns^{-1}, $\tau = 3$ ns. For these parameters, without coupling the lasers emit the x polarization. The angular frequency detuning between the two polarizations, δ, and the coupling strength, η, will be considered as control parameters.

A. Stable square-wave switching in the parameter space (η, δ)

For each set of parameters (η, δ) we integrated a trajectory, starting from initial conditions with both lasers off, until a stable output was reached (and the trajectory approached one of the model fixed points), or the maximum integration time was reached, 6 μs. Figure 1(a) presents in gray color code the stationary state of the coupled lasers as a function of η and δ. MM/PM indicates mixed-mode or pure-mode steady state; PO/IO indicates periodic or irregular oscillations and SW indicates regular square wave switching.

The lifetime of the transient dynamics is plotted in gray color code in Fig. 1(b) and is defined as the time interval during which the amplitude of the fluctuations of the intensity of the x polarization of both lasers, measured in terms

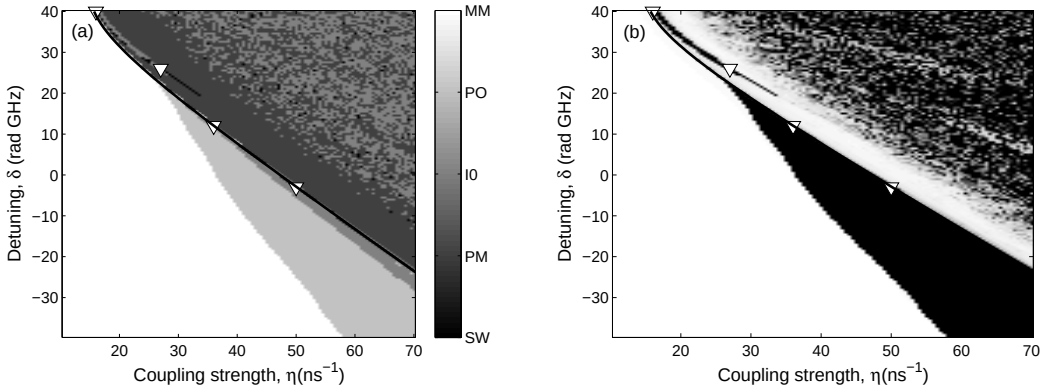

FIG. 1. (a) Phase diagram in the parameter space (coupling strength, detuning). The gray color scale indicates the stationary behavior, from white to black: mixed-mode solution (MM), periodic oscillations (PO), irregular oscillations (IO), pure-mode solution (PM) and square-wave switching (SW). The black line displays the solution of Eq. (18) and the triangles, the parameters of Figs. 2 (a)-(d). (b) Duration of the transient time, in gray scale (white: a few tens of ns, black: 6 μs). The parameters are as indicated in the text.

of the standard deviation calculated in a time window, is above a certain value (4% of the average intensity). In other words, we considered that the transient dynamics finished when either the fluctuations of I_{1x} or I_{2x} are below the threshold; if at the end of the simulation the dynamics of the coupled lasers is such that I_{1x} and I_{2x} are both still time dependent, with oscillations larger than the threshold, then, the duration of the transient is considered to be equal to the integration time (6 μs).

While the mixed-mode solution is usually reached very fast, the transient towards the pure-mode solution tends to be much longer and depends on the noise level, as will be discussed latter. In Fig. 1(a), regular square-waves (black dots) occur in several very narrow parameter regions that are located very close to the boundary of stability of the pure-mode solution [in Fig. 1(a) the black line indicates the solution of Eq. (18), i.e., the location of the transcritical bifurcation in the parameter plane (η, δ)]. Much longer simulations with parameters chosen in these narrow windows reveal that the square-waves are indeed stable. A few examples of the waveforms are displayed in Fig. 2 that plots the time traces of the intensities, I_x and I_y, of one of the lasers (the corresponding parameters are indicated with triangles in Fig. 1).

Many black dots that are randomly scattered within the region of stability of the pure-mode [top-right corner in Fig. 1(a)] represent also regular square-waves; however, in this parameter region longer simulations reveal that the square-waves are a transient dynamics that eventually finishes when the pure-mode is found.

While in Ref. [17] stable square-waves were found only in a narrow range of negative detuning values, in Fig. 1(a) we can observe that they also occur at certain positive values of δ. In the various narrow regions of square-wave switching, the shape of the square-waves can change considerably, as shown in Fig. 2. This suggests that the square-waves in different regions might originate from different sequences of bifurcations of the mixed-mode solution.

Outside the narrow windows of stable switching and near the boundary of stability of the pure-mode solution, the stationary dynamics, after a long square-wave switching transient, tends to the emission of pulses with orthogonal polarizations: one laser emits the x polarization and with certain periodicity emits one or more pulses in the y polarization; while the other laser emits the y polarization and, also with the same periodicity, emits one or more pulses in the x polarization.

B. Influence of gain saturation and noise

In Ref. [17] the square waves were found for a specific set of the gain saturation coefficients (such that $\epsilon_{xx} < \epsilon_{xy} < \epsilon_{yx} < \epsilon_{yy}$). Here we have done a detailed analysis of the parameter space (δ, η) varying also the gain saturation coefficients and found that stable square waves occur indeed in narrow regions but for many combinations of the gain saturation coefficients, including when they are all equal, as shown in Figs. 3 and 4. In fact, we found that in order to observe stable square waves there is no need to include gain saturation in the model, and these are seen in narrow regions, also with $\epsilon_{xx} = \epsilon_{xy} = \epsilon_{yx} = \epsilon_{yy} = 0$ (Fig. 5); however, without gain saturation the square-waves display more undamped fast pulsations at the relaxation oscillation frequency. A few examples of waveforms are displayed in Fig. 6.

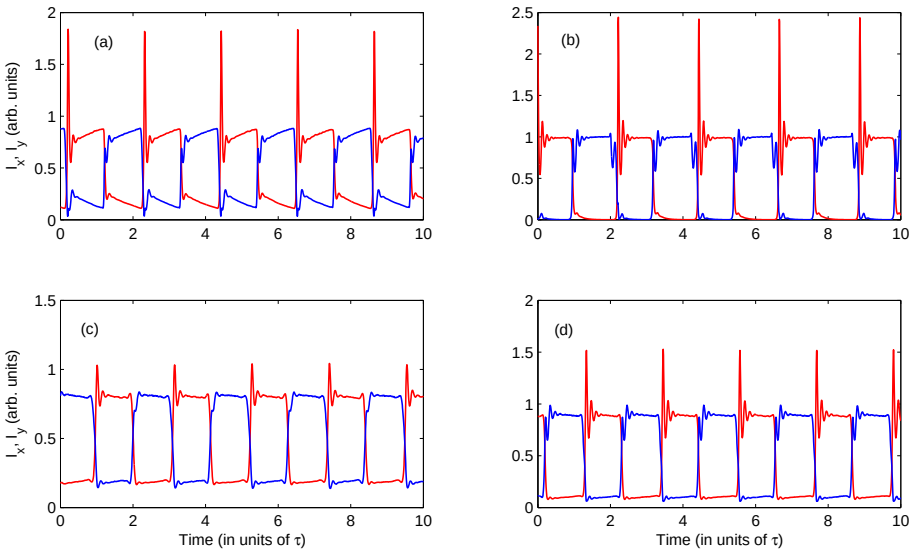

FIG. 2. Stable square-wave solutions. The x (red) and y (blue) intensities of one laser are plotted versus time. The parameters are (indicated with triangles in Fig. 1): $\eta = 16$ ns^{-1}, $\delta = 40$ rad GHz (a); $\eta = 27$ ns^{-1}, $\delta = 26$ rad GHz (b); $\eta = 36$ ns^{-1}, $\delta = 12$ rad GHz (c); $\eta = 50$ ns^{-1}, $\delta = -3$ rad GHz (d).

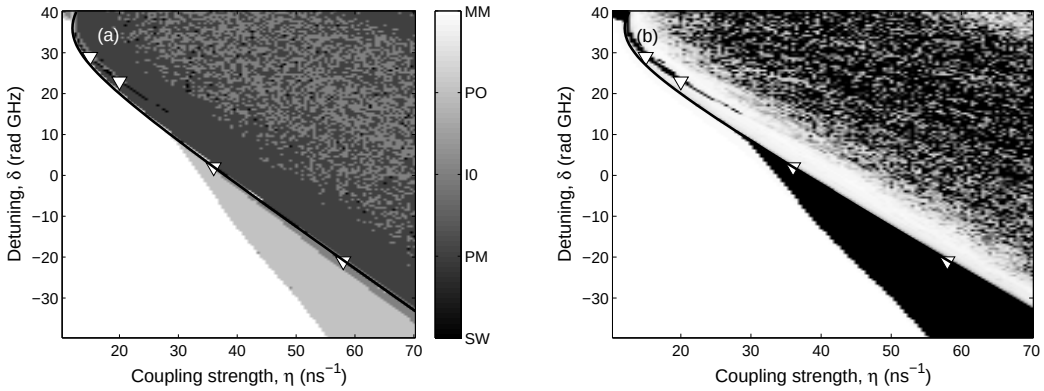

FIG. 3. Stationary dynamics in the parameter space (coupling strength, angular frequency detuning) (a) and duration of the transient time (b). The gray color code is the same as in Fig. 1, the black line displays the solution of Eq. (18), and the triangles indicate the parameters of Figs. 4 (a)-(d). The gain saturation coefficients are all equal ($\epsilon_{xx} = \epsilon_{xy} = \epsilon_{yx} = \epsilon_{yy} = 0.01$), and other parameters are as indicated in the text.

The wave form in Fig. 6(a), for fixed detuning $\delta = 26$ rad GHz is stable in the range of coupling strengths 14.5 ns^{-1} $< \eta <$ 15.5 ns^{-1}. In this range the waveform maintains the quasiperiodic structure of fast relaxation oscillations modulated by the slower coupling delay time. This waveform is found below the boundary of instability of the pure mode solution (at $\eta = 15.5$ ns^{-1} for $\delta = 26$ rad GHz) and we did not find coexistence of the two solutions.

The wave forms displayed in Figs. 6(b) and 6(c) are stable within a range of (η, δ) values that is wider than the typical intervals where stable square waves are found. In spite of the fact that this range of values is embedded in the region of stability of the pure-mode solution, we could not find, trying with different initial conditions, any coexistence of stable square waves and the pure mode solution.

The wave form displayed in Fig. 6(d) is stable in the small range 45.76 ns^{-1} $< \eta <$ 46.15 ns^{-1} for $\delta = -8$ rad GHz and coexists with similar other waveforms that can be captured by using different initial conditions. For $\eta >$ 46.15 ns^{-1} the square waves decay to the pure mode after long transients.

Thus, to summarize, the above presented results demonstrate that, although the intervals of coupling strengths where there are stable square-waves are usually narrow, they occur for quite different combinations of parameters,

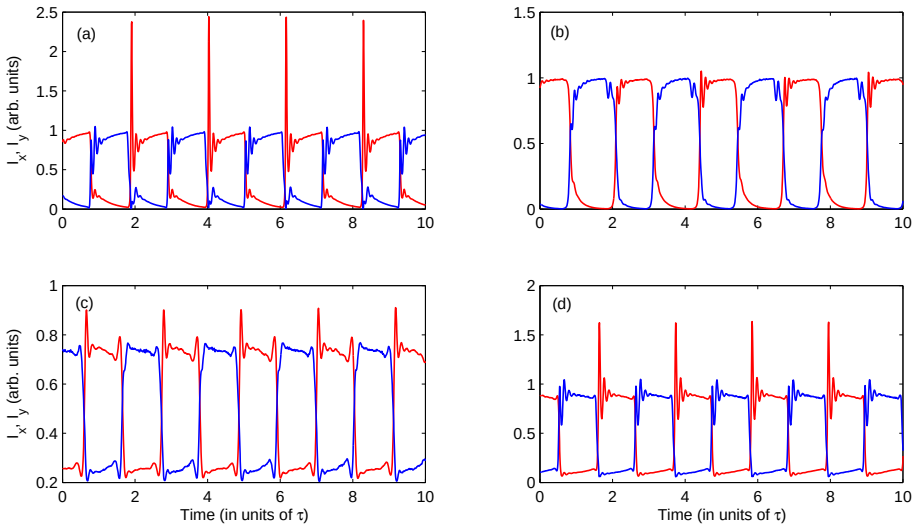

FIG. 4. Square-wave switching when the gain saturation coefficients are all equal to 0.01. The coupling and detuning parameters are (indicated with triangles in Fig. 3): $\eta = 15$ ns^{-1}, $\delta = 29$ rad GHz (a); $\eta = 21$ ns^{-1}, $\delta = 22$ rad GHz (b); $\eta = 36$ ns^{-1}, $\delta = 2$ rad GHz (c); $\eta = 58$ ns^{-1}, $\delta = -21$ rad GHz (d).

and thus we can expect that their existence explains the measurements in [16, 17], and confirms the stability of the experimental observed square-wave forms.

However, an important issue in the stability of the numerical solutions is the role of noise. The results of deterministic simulations (setting $\beta_{sp} = 0$), presented in Figs. 7 and 8 for the same parameters as Figs. 1 and 5 respectively, demonstrate that the narrow regions of stable square-waves persist. As expected from the analysis of Ref. [18], the stable square-waves are not supported and do not need the addition of noise. One can also notice, by comparing Figs. 7(b), 8(b) with 1(b) and 5(b) that the duration of the transient dynamics towards the pure-mode solution is significantly shorter in the absence of noise, while the duration of the transient towards the mixed-mode is almost unaffected.

Since the transient dynamics towards the pure-mode consists of square-wave switchings that gradually become irregular, it is also possible that the square-waves observed experimentally in [16, 17] are in fact a transient induced by the presence of noise. "Deterministic" stable square-wave switching occurs in such narrow parameter regions that in fact these regions can be considered as experimentally unreachable.

It is also worth noticing that a comparison of Fig. 7 with Fig. 1 reveals that in the absence of noise, no additional regions of stable square waves are seen; i.e. the simulations without noise presented in Fig. 7 do not reveal square waves that were not already found in the stochastic simulations presented in Fig. 1. On the contrary, when the simulations are done with $\epsilon_{xx} = \epsilon_{xy} = \epsilon_{yx} = \epsilon_{yy} = 0$, as seen in Fig. 8, the noise-free simulations reveal several new regions of stable square waves, as compared to those in Fig. 5. These regions are located inside the region where the pure mode solution is stable. Deterministic simulations starting with different initial conditions reveal that these waveforms are indeed stable; however, in the stochastic simulations, small fluctuations allow the trajectory to eventually find the coexisting stable pure-mode solution. Thus, while for most parameters within the region of stable pure-mode the inclusion of noise results in long, square-wave switching transients (as compared to deterministic simulations), for certain parameters, noise has the opposite effect. In noiseless simulations there is stable square-wave switching while in stochastic simulations, the switching is a transient and the trajectory eventually finds the pure mode (that is not found in the absence of noise).

IV. CONCLUSIONS

To conclude, we performed a detailed analysis of square-wave polarization switching in two semiconductor lasers with time-delayed, orthogonal mutual coupling. We found that the general behavior of the system is as follows: low enough coupling the mixed-mode fixed-point is stable (in this state the two lasers emit the two polarizations simultaneously); while for high enough coupling the pure-mode fixed-point is stable (in this state the two lasers emit

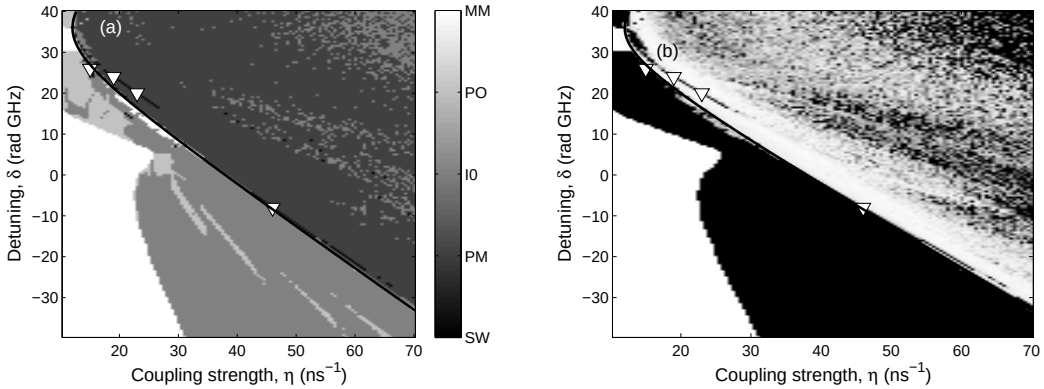

FIG. 5. As Figs. 1 and 3 but without gain saturation ($\epsilon_{xx} = \epsilon_{xy} = \epsilon_{yx} = \epsilon_{yy} = 0$). The black line displays the solution of Eq. (18) and the triangles indicate the parameters of Figs. 6 (a)-(d).

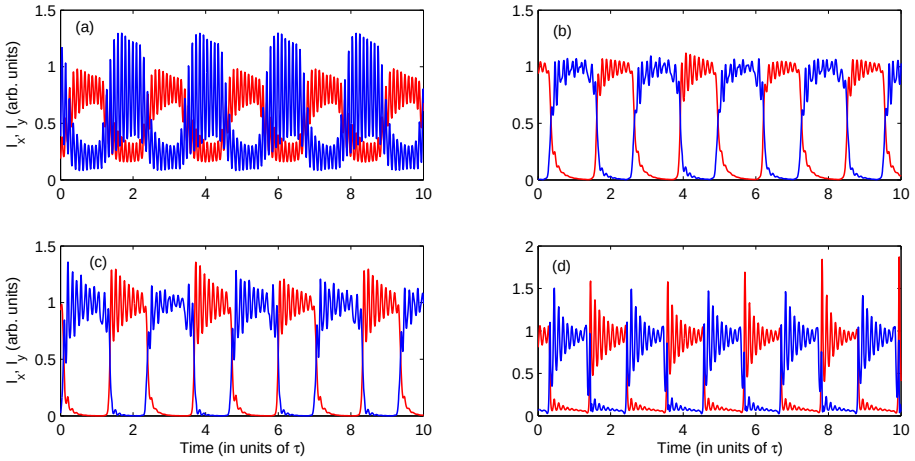

FIG. 6. Square-wave-like switching when in the simulations the gain saturation coefficients are set equal to 0. The coupling and detuning parameters are (indicated with triangles in Fig. 5): $\eta = 15$ ns^{-1}, $\delta = 26$ rad GHz (a); $\eta = 19$ ns^{-1}, $\delta = 24$ rad GHz (b); $\eta = 23$ ns^{-1}, $\delta = 20$ rad GHz (c); $\eta = 46$ ns^{-1}, $\delta = -8$ rad GHz (d).

orthogonal polarizations). In between these two regions there are time-depend solutions that arise from bifurcations of the pure-mode or of the mixed-mode. Stable square-wave switching was found in very narrow parameter regions that were located near the boundary of stability of the pure mode solution. In these narrow regions we found different types of square wave forms and carefully checked their stability. Our results show that, in the simpler model without nonlinear gain, stable square waves also occur in narrow parameter regions, and exhibit a fast weakly damped oscillation at the relaxation frequency of the laser in addition to the fundamental modulation at the coupling delay time. Finally, we studied the influence of noise and showed that it usually (but not always) enlarges the duration of the square-wave switching transient as compared to deterministic simulations.

We found numerically that there are many parameter intervals where there are stable square-waves, and these intervals occur for quite different combinations of parameters. Thus, we could speculate that our results explain the square-wave forms experimentally measured in Refs. [16, 17], or confirm their stability. However, since noise induces long, square-wave transient dynamics towards the pure-mode, it is also possible that the waveforms observed experimentally were in fact noise-induced, because the "deterministic" and stable square-waves (that do not need the inclusion of noise) occur in such narrow parameter regions that in fact these regions could be considered as experimentally unreachable. Thus, we hope that our results will motivate new experimental studies with focus on the statistical properties of the switchings, that would allow clarifying this issue, if they are a deterministic, or a noise-sustained dynamics.

For future work, to yield light into this issue, it would be interesting to analyze the polarization switching dynamics employing nonlinear methods of time series analysis, such as ordinal analysis [19, 20]. Varying the laser pump current

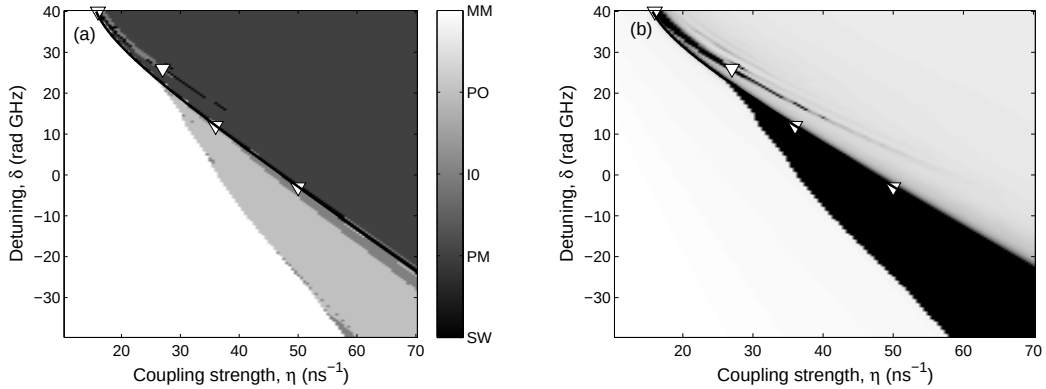

FIG. 7. As Fig. 1 but with no noise included in the simulations. The black line displays the solution of Eq. (18) and the triangles indicate the parameters of Figs. 2 (a)-(d).

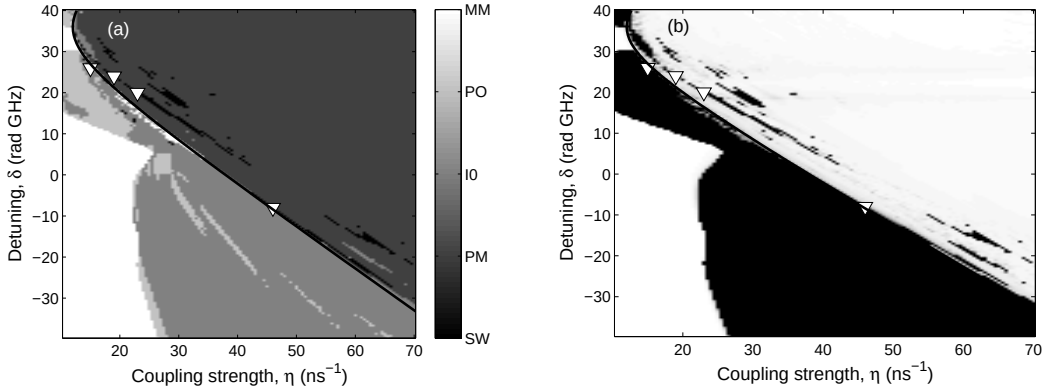

FIG. 8. As Fig. 5 but with no noise included in the simulations. The black line displays the solution of Eq. (18) and the triangles indicate the parameters of Figs. 6 (a)-(d).

(a parameter that can be easily controlled experimentally) would allow exploring the parameter region close to the laser threshold, where a stronger influence of noise could be expected, as compared to the region that has been studied so far, which is above twice the threshold [16–18].

CM acknowledges the support of the Spanish Ministerio de Ciencia e Innovacion through Project No. FIS2009-13360-C03-02, the AGAUR, Generalitat de Catalunya, through Project No. 2009 SGR 1168, EOARD Grant No. FA8655-12-1-2140, and the ICREA Academia programme. MS acknowledges the support of Conseil Regional de Lorraine, of the ANR (Agence Nationale de la Recherche) through the TINO JCJC research project, and of the Interuniversity Attraction Poles program of the Belgian Science Policy Office, under grant IAP P7-35 photonics@be.

[1] D. M. Kane and K. A. Shore, *Unlocking dynamical diversity: optical feedback effects on semiconductor lasers* (Wiley, 2005).
[2] L. Larger, J.-P. Goedgebuer, and J.-M. Merolla, "Chaotic oscillator in wavelength: A new setup for investigating differential difference equations describing nonlinear dynamics", IEEE J. Quantum Electron. **34**, 594 (1998).
[3] T. Erneux, L. Larger, M. W. Lee, J.-P. Goedgebuer, "Ikeda Hopf bifurcation revisited", Physica D **194**, 49 (2004).
[4] Y. Chembo Kouomou, P. Colet, L. Larger, and N. Gastaud, "Chaotic breathers in delayed electro-optical systems", Phys. Rev. Lett. **95**, 203903 (2005).
[5] M. Sciamanna, P. Mégret, and M. Blondel, "Hopf bifurcation cascade in small-alpha laser diodes subject to optical feedback", Phys. Rev. E **69**, 046209 (2004).
[6] L. Larger, J.-P. Goedgebuer, and T. Erneux, "Subcritical Hopf bifurcation in dynamical systems described by a scalar nonlinear delay differential equation", Phys. Rev. E **69**, 036210 (2004).
[7] S. Jiang, Z. Pan, M. Dagenais, R. A. Morgan, K. Kojima, "High-frequency polarization self-modulation in vertical-cavity surface emitting lasers", Appl. Phys. Lett. **63**, 3545 (1993).

[8] F. Robert, P. Besnard, M. L. Charès, G. Stéphan, "Polarization modulation dynamics of vertical-cavity surface-emitting lasers with an extended cavity", IEEE J. Quantum Electron. **QE-33**, 2231 (1997).
[9] H. Li, A. Hohl, A. Gavrielides, H. Hou, and K. D. Choquette, "Stable polarization self-modulation in vertical-cavity surface-emitting lasers", Appl. Phys. Lett. **72**, 2355 (1998).
[10] M. Sciamanna, T. Erneux, F. Rogister, O. Deparis, P. Mégret, and M. Blondel, "Bifurcation bridges between external-cavity modes lead to polarization self-modulation in vertical-cavity surface-emitting lasers", Phys. Rev. A **65**, 041801(R) (2002).
[11] M. Sciamanna, F. Rogister, O. Deparis, P. Mégret, M. Blondel, and T. Erneux, "Bifurcation to polarization self-modulation in vertical-cavity surface-emitting lasers", Opt. Lett. **27**, 261 (2002).
[12] T. Heil, A. Uchida, P. Davis, and T. Aida, "TE-TM dynamics in a semiconductor laser subject to polarization-rotated optical feedback", Phys. Rev. A **68**, 033811 (2003).
[13] A. Gavrielides, T. Erneux, D. W. Sukow, G. Burner, T. McLachlan, J. Miller, and J. Amonette, "Square-wave self-modulation in diode lasers with polarization-rotated optical feedback", Opt. Lett. **31**, 2006 (2006).
[14] A. Gavrielides, D. W. Sukow, G. Burner, T. McLachlan, J. Miller, and J. Amonette, "Simple and complex square waves in an edge-emitting diode laser with polarization-rotated optical feedback", Phys. Rev. E **81**, 056209 (2010).
[15] L. Mashal, G. Van der Sande, L. Gelens, J. Danckaert, and G. Verschaffelt, "Square-wave oscillations in semiconductor ring lasers with delayed optical feedback", Optics Express **20**, 22503 (2012).
[16] D. W. Sukow, A. Gavrielides, T. Erneux, B. Mooneyham, L. Lee, J. McKay, J. Davis, "Asymmetric square waves in mutually coupled semiconductor lasers with orthogonal optical injection", Phys. Rev. E **81**, 025206(R) (2010)
[17] C. Masoller, D. W. Sukow, A. Gavrielides, M. Sciamanna, "Bifurcation to square-wave switching in orthogonally delay-coupled semiconductor lasers: Theory and experiment", Phys. Rev. A **84**, 023838 (2011).
[18] M. Sciamanna, M. Virte, C. Masoller, A. Gavrielides, "Hopf bifurcation to square-wave switching in mutually coupled semiconductor lasers", Phys. Rev. E **86**, 016218 (2012).
[19] C. Masoller, O. A. Rosso, "Quantifying the complexity of the delayed logistic map", Phil. Trans. R. Soc. A **369** 425 (2011).
[20] N. Rubido, J. Tiana-Alsina, M. C. Torrent, J. Garcia-Ojalvo, C. Masoller, "Language organization and temporal correlations in the spiking activity of an excitable laser: Experiments and model comparison", Phys. Rev. E **84**, 026202 (2011).